

Article

Evaluation of Fatty Acid Methyl Esters (FAME) as a Green Alternative to Common Solvents in Conservation Treatments

Camilla Zaratti ^{1,2,*}, Livia Marinelli ^{1,3} , Irene Angela Colasanti ^{1,2,4}, Francesca Irene Barbaccia ^{1,5}, Helene Aureli ¹ , Fernanda Prestileo ⁶, Tilde de Caro ⁷ , Mauro Francesco La Russa ⁸ and Andrea Macchia ^{1,8} 

¹ YOCOCU APS—Youth in Conservation of Cultural Heritage, Via T. Tasso 108, 00185 Rome, Italy; livia.marinelli@uniroma1.it (L.M.); ireneangela.colasanti@students.uniroma2.ue (I.A.C.); francescairene.barbaccia@uninettuniversity.net (F.I.B.); andrea.macchia@unical.it (A.M.)

² Lab4green s.r.l, Via T. Tasso 108, 00185 Rome, Italy

³ Department of Science of Antiquities, Sapienza University of Rome, Piazzale Aldo Moro 5, 00185 Rome, Italy

⁴ Chemical Sciences Technologies Department, Tor Vergata University of Roma, Via della Ricerca Scientifica 1, 00133 Rome, Italy

⁵ Department of Technological Innovation Engineering, Digital Technologies for Industry 4.0, Uninettuno University, Corso Vittorio Emanuele II 39, 00186 Rome, Italy

⁶ CNR-ISAC, Institute of Atmospheric and Climate Sciences, Via Fosso del Cavaliere 100, 00133 Rome, Italy; fernanda.prestileo@cnr.it

⁷ CNR ISMN, Institute for the Study of Nanostructured Materials, Strada Provinciale 35d, 9, 00010 Rome, Italy; tilde.decaro@cnr.it

⁸ Department of Biology, Ecology and Earth Sciences (DIBEST), University of Calabria, Via Pietro Bucci, Arcavacata, 87036 Rende, Italy; mlarussa@unical.it

* Correspondence: camilla.zaratti@lab4green.it

Abstract: This study investigates the potential of fatty acid methyl esters (FAME) as environmentally sustainable alternatives to traditional solvents for the removal of low-polarity materials commonly found in cultural heritage artefacts. Recognizing the environmental and health concerns associated with conventional solvents, this research focuses on FAME to remove low/non-polarity or non-polar substances used in cultural heritage preservation. Laboratory samples coated with low molecular synthetic resins (LMW) such as Regalrez 1094 and microcrystalline wax were treated with FAME applied in gel to prevent solvent–substrate interactions. Photographic documentation under UV-vis light, optical microscope observations, and spectrophotometric analysis were used for assessing surface “cleanness”, while FTIR-ATR spectroscopy was used to detect possible residue from treatment. Moreover, SEM analysis was used for a better understanding of the results. The best results were obtained using FAME base on methyl stearate according to Hansen-RED.

Keywords: green solvents; fatty acid methyl esters (FAME); cleaning; low/non-polar substances; cultural heritage conservation



Citation: Zaratti, C.; Marinelli, L.; Colasanti, I.A.; Barbaccia, F.I.; Aureli, H.; Prestileo, F.; de Caro, T.; Russa, M.F.L.; Macchia, A. Evaluation of Fatty Acid Methyl Esters (FAME) as a Green Alternative to Common Solvents in Conservation Treatments. *Appl. Sci.* **2024**, *14*, 1970. <https://doi.org/10.3390/app14051970>

Academic Editor: Simone Morais

Received: 30 January 2024

Revised: 21 February 2024

Accepted: 22 February 2024

Published: 28 February 2024



Copyright: © 2024 by the authors. Licensee MDPI, Basel, Switzerland. This article is an open access article distributed under the terms and conditions of the Creative Commons Attribution (CC BY) license (<https://creativecommons.org/licenses/by/4.0/>).

1. Introduction

The conservation of cultural heritage requires meticulous approaches to preserving artworks, often relying on organic solvents for various restoration and maintenance tasks. Most of the solvents used, while effective, have raised concerns regarding their environmental impact and adverse health effects on conservators [1,2]. Today it has become imperative to commit to sustainable conservation practices, in line with global initiatives such as the EU Green Deal and Agenda 2030.

Organic solvents play a multifaceted role in cultural heritage conservation, from surface cleaning and protective coating to adhesive dilution and organic matter removal [3–7]. An unresolved challenge in this domain pertains to the removal of substances exhibiting low polarity or non-polar characteristics [8,9]. Solvents commonly used for their removal [10,11] pose considerable environmental and health risks, particularly in the case of material such

as microcrystalline waxes, which are widely employed as protective coatings for the substrate of diverse artworks [12–17].

In response to the escalating demand for sustainable practices, various new strategies for removing low/non-polar substances have been studied [18–21]. Recently, fatty acid methyl esters (FAME) are being studied as a potential green solvent. These compounds have emerged as promising candidates to replace low-polarity solvents due to their biodegradability, minimal volatile organic compound (VOC) emission, and non-toxic nature [22,23]. Synthesized through alkali-catalysed reactions involving fats and methanol [24], the fatty acid chains comprise carbon chain lengths ranging from C6 (e.g., methyl hexanoate, CAS 106-70-7) to C18 (e.g., methyl stearate, CAS 112-61-8), mainly saturated but also mono- and di-unsaturated C18 (e.g., methyl oleate, CAS 112-62-9 and methyl linoleate, CAS 112 63 0).

The present study endeavours to explore the potential of FAME as an alternative solvent for removing low-polarity materials commonly used as in-painting media and picture varnishes like low molecular weight (LMW) synthetic resins (Regalrez 1094) and microcrystalline wax [25,26].

The aim of the experiment was to evaluate the effectiveness of FAME in removing the aforementioned low-polar substances. FAME were applied to the surface of prepared laboratory mock-ups (four canvases coated with two different types of non-polar coatings: microcrystalline wax and Regalrez 1094 varnish) using a gel formulation due to their negligible or low volatility, thus addressing the need to prevent solvent–substrate interactions in cultural heritage applications. The cleaning efficacy was assessed on the laboratory samples utilizing the following analytical techniques: visible (vis) and ultraviolet (UV) imaging, digital microscope observations, spectrophotometry, Fourier-transform infrared (FTIR) spectroscopy, and scanning electron microscopy (SEM).

In cleaning restoration practice, an important step (and the first that should be carried out) is the evaluation and choice of the most suitable solvent in order to assess different parameters; namely, assessing compatibility with the artwork's constituent materials, finding the solvent with the most suitable strength to remove the substances in question, and avoiding unwanted solvent–substrate interactions. The prevalent tool among conservators for solvent evaluation and identification of potential eco-friendly alternatives is the Teas Chart [27]. Although the Teas Chart is characterized by several limitations pertaining to solute–solvent interaction phenomena like leaching and swelling and by its inability to address substance solubility under varying pH conditions [28], for the conservator, it represents an invaluable resource. The solvent power is described on a triangular graphic using the three Hansen solubility parameters (δ d: dispersion forces; δ p: polar forces; and δ h: hydrogen bonding). According to the Teas Chart, the area for wax (non-polar material) is located at the lower right corner. Petroleum ether, toluene, and xylene were placed in the Teas Chart in the same area of waxes, and hence were used as solvent for them. Due to the toxicity of toluene and xylene, mineral spirits and ligroin were selected during experimentation as reference solvents used in the removal of microcrystalline wax and Regalrez 1094 varnish.

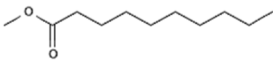
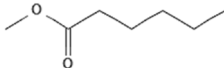
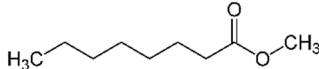
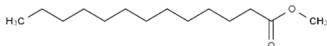
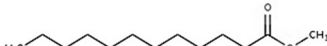
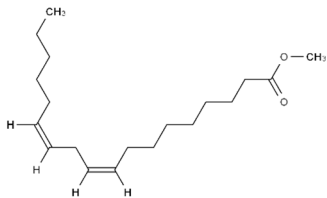
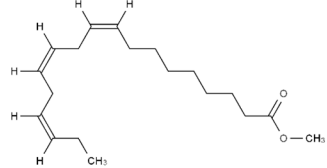
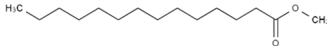
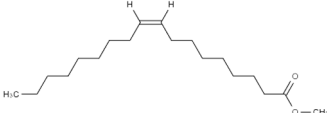
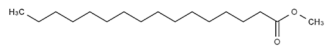
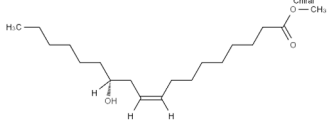
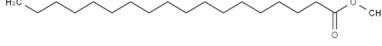
The findings indicate that FAME could be a suitable alternative to common toxic solvents used in cultural heritage restoration practices, providing a level of cleaning comparable to reference toxic solvents (i.e., white spirits and ligroin) while respecting the health of the operator and the integrity of the artwork.

2. Materials and Methods

2.1. FAME Selection

The list of FAME available on the ECHA website (<https://echa.europa.eu/it/registration-dossier/-/registered-dossier/15897/7/2/1>) (accessed on 23 September 2023) was examined in order to choose potential FAME to employ in the experiment. Table 1 presents a list summary of FAME found on the ECHA website, reporting their name, their formula, and when available, the compound structure.

Table 1. List of FAME.

Compound Name	Formula	Structure
Methyl Canolate	$\text{CH}_3(\text{CH}_2)_{10}\text{CO}_2\text{CH}_2\text{CH}_2\text{SO}_3\text{Na}$	-
Methyl Caprate (Methyl decanoate)	$\text{C}_{11}\text{H}_{22}\text{O}_2$	
Methyl Caproate (Methyl hexanoate)	$\text{C}_7\text{H}_{14}\text{O}_2$	
Methyl Capylate (Octanoate)	$\text{CH}_3(\text{CH}_2)_6\text{CO}_2\text{CH}_3$	
Methyl Cocinate	$\text{C}_{14}\text{H}_{28}\text{O}_2$	
Methyl Laurate (Methyl Dodecanoate)	$\text{C}_{13}\text{H}_{26}\text{O}_2$	
Methyl Linoleate	$\text{C}_{19}\text{H}_{34}\text{O}_2$	
Methyl Linolenate	$\text{C}_{19}\text{H}_{32}\text{O}_2$	
Methyl Myristate (Methyl tetradecanoate)	$\text{C}_{15}\text{H}_{30}\text{O}_2$	
Methyl Oleate (Methyl (Z)-9-Octadecenoate)	$\text{C}_{19}\text{H}_{36}\text{O}_2$	
Methyl Palmitate	$\text{C}_{17}\text{H}_{34}\text{O}_2$	
Methyl Ricinoleate	$\text{C}_{19}\text{H}_{36}\text{O}_3$	
Methyl Stearate	$\text{C}_{19}\text{H}_{38}\text{O}_2$	
Methyl Soyate	Fatty acids C16–18.	-

The solubility parameters were evaluated from the list of FAME shown in Table 1, starting with the Hansen solubility parameters (HSPs). The cohesive energy or HSPs of FAME were computed using the commercial software HSPiP 6.0, and they were based on two methods: the van Krevelen–Hoftyzer approach and the Stefanis and Panayiotou approach [29,30].

The former, based on the additive theory of functional group contributions, computes the solubility parameter components (δ_d , δ_p , and δ_h) from group force contributions

using a first-order equation. Meanwhile, the latter employs a second-order equation to achieve greater accuracy in determining these parameters. The average between FAME van Krevelen–Hoftyzer and Stefanis and Panayiotou solubility parameters was transformed into Teas parameters that are mathematically derived from Hansen values using the following equations by allowing a 2D view of 3D data:

$$F_d = \delta d / \delta d + \delta p + \delta h; \quad F_p = \delta p / \delta d + \delta p + \delta h; \quad F_h = \delta h / \delta d + \delta p + \delta h$$

$$F_d + F_p + F_h = 100$$

where F_d is the dispersion component of the fractional cohesion, F_p is the polar component, and F_h is the hydrogen bonding.

From the list of FAME presented in Table 1, six pure FAME were then selected based on the Teas Chart and compared to Ligroin and Mineral spirits (which were taken as reference solvent), respectively employed as common solvent for the removal of microcrystalline wax and varnish called “Regalrez 1094”. These were further compared to a commercially available FAME product consisting of a blend of methyl esters (Agnique® ME).

2.2. Laboratory Samples

Two non-polar materials, microcrystalline wax and Regalrez 1094 varnish, were applied to two types of substrates—commercial canvases coated with red acrylic paint and red pigment dispersed in linseed oil, respectively. A total of four canvases were prepared. The choice of these sample types was driven by the necessity to understand potential interactions between FAME and common substrates prevalent in the realm of cultural heritage, such as oil paintings or contemporary acrylic artworks.

The decision to craft laboratory samples in this manner stemmed from the fact that the solubility parameters of FAME coincide with the swelling and leaching areas of supports made with acrylic and linseed oil. Stone materials were disregarded due to their high polarity, which precludes such interactions. Paint layers were aged to simulate conditions akin to real scenarios, following the ageing by SUNTEST method for 144 h [31]. A uniform layer of non-polar coating was applied atop the prepared paint layers. To facilitate the macroscopic tracking of cleaning on both varnishes, Fe_3O_4 was introduced as a marker.

2.3. FAME Application

The laboratory samples were divided on to nine squares of the same dimension (5×5 cm). Due to the interaction with the substrate, for the application a gel formulation was prepared. A homogenous solution was prepared by using poly-hydroxybutyrate (PHB); the polymer was stirred at $50^\circ C$ for 6 h. This polymer was chosen because in previous studies, this bioderived-based polymer has been used within a similar scope [32,33].

The FAME were added to the polymer, and the formulation was cooled at room temperature for two hours. Figure 1 shows the placement of the different FAME gels on the laboratory samples. Starting from the upper left corner, the succession of the different FAME gels that were formulated is placed from top to bottom.

The gels formulated with the reference solvent (ligroin for microcrystalline wax and white spirit for “Regalrez 1094” varnish) were placed on the top left corner and marked as Gel 1. In the square at the top right corner, the gel formulation prepared with only the polymer was placed (named Gel 9) to assess the possible solubility powder of the polymer.

The cleaning process involved direct application of gels onto the surface of canvases treated with non-polar varnishes, allowing a five-minute contact time. Eventually, residues of gel formulations present on the surface were subsequently removed by rolling a dry cotton swab across the cleaned surface. Upon repeating the application on the surface, the areas were found to be completely clean. However, the repeated application led to the interaction between the gels and the paint layer.

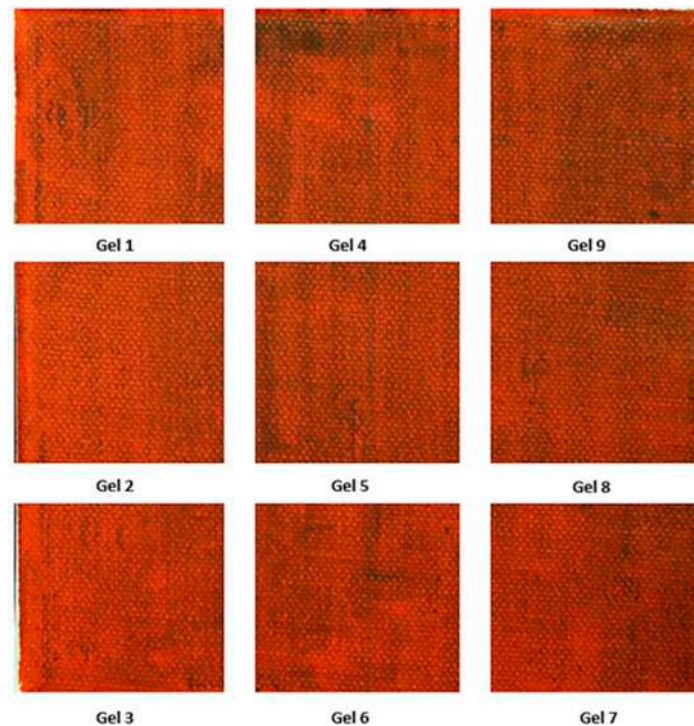


Figure 1. Placement of the FAME gels on the prepared laboratory samples.

2.4. Efficacy of Cleaning Test

To define the effectiveness to remove the varnish and microcrystalline wax, targeted analytical methods were employed:

- UV-vis imaging was conducted to macroscopically assess the efficacy of cleaning using various FAME. Visible and UV light imaging was employed to capture crucial data regarding surface layer conditions and the extent of varnish removal. Imaging was performed on the canvas using a CANON EOS M50, Canon, Tokyo, Japan full spectrum camera equipped with specific filters: the HOYA UV-IR (Madatec, Milan, Italy) cut filter 52 and Yellow 495 52 mm F-PRO MRC 022 (Madatec, Milan, Italy) even though the camera was positioned as parallel as possible to the surface some reflection of the varnish can still be seen. For each FAME, the removal area ratio was calculated by processing acquired images: the percentage of the residues area (in black) to the entire sample area of the cleaning test. The percentage of the black area was determined used Photoshop Adobe (v.CS6) software to identify the pixels with the different colour in the picture, using a tolerance of 5% (Figure 2). The image was rasterized at 600 DPI and subsequently, its histogram was analysed using Photoshop. The obtained value was divided by 255 and then subtracted from 1. This process allowed for obtaining the percentage of black normalized to 1 (where 1 represents 100% black and 0 represents 0% black). Additionally, the values of clean areas were normalized based on the values obtained from the same areas in the untreated canvas, as shown below.
- A DinoLite AM411-FVW digital microscope (Leica Microsystems, Wetzlar, Germany) operating at 40 and 220 magnifications in both visible (VIS) and ultraviolet (UV) light modes was used to observe surface morphology.
- Spectrocolorimetry was conducted using the YS3010 3nh Handheld Spectrophotometer (Shenzhen ThreeNH Technology Co., Ltd, Shenzhen, China) to define the colour surface difference before and after the cleaning treatments, using the total colour variation (ΔE) as a quantitative index to evaluate cleanliness. ΔE was calculated as the difference between the colour parameters of the surfaces following cleaning treatment and those of the surfaces both without the application of crystalline wax and Regarlez

1094 varnish and with the application of the two coatings. To facilitate the analysis of colorimetric data, emphasis has been placed on calculating chromatic variation concerning the surface obtained after the cleaning treatment in comparison with the painted surface and the surface coated with Regarlez or microcrystalline wax. For this purpose, the following index has been computed:

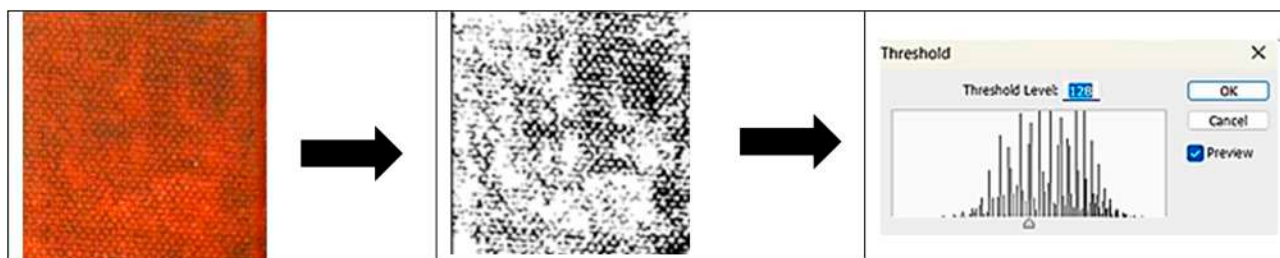


Figure 2. The step in the process of calculating the percentage of black present on the surface of canvases.

$$v = \frac{\Delta E (\text{Surface after the cleaning Treatment} - \text{Painting surface})}{\Delta E (\text{Surface Surface after the cleaning Treatment} - \text{Surface with the wax/Regarlez coating})}$$

Colorimetric data were collected from the same regions of the painted canvas, treated with both types of varnish, and cleansed (five areas divided into a central zone and four corners). The data represent an average of measurements collected from the following areas.

- To confirm the absence or presence of surface residues, Fourier-transform infrared (FTIR) spectroscopy in attenuated total reflection (ATR) mode was performed using the Nicolet Summit Pro instrument from Thermo Scientific (Waltham, MA, USA). The areas that appeared macroscopically clean were brought into contact with the instrument's diamond. Spectra were acquired in the range of 400–3200 cm^{-1} , with a total of 32 scans at a resolution of 4 cm^{-1} ;
- Scanning electron microscopy (Tescan Vega model) was performed to better understand the interaction between the non-polar coating and the underlying pictorial layer. The SEM observations were obtained by appropriately varying the instrumental parameters with an electron beam potential of 30 KeV by using the secondary electron detector for a definition of the surface morphology but also, in some cases, by using the coupling with backscattered electron vision. In this way, it is possible to exploit the atomic number contrast in backscattered electrons, allowing for the identification of different surface compositions from the grey gradient.

3. Results

3.1. FAME Selection

Table 2 reports the value of Hansen and Teas parameters for the FAME shown in Table 1. The increment in the CH_2 groups within the ester molecule directly associates with an increase in the dispersion solubility parameter (δD) due to heightened van der Waals intermolecular forces. Moreover, distinct structural features intrinsic to different fatty acid esters result in further disparities. Factors such as chain length, levels of unsaturation, and branching exert substantial influence over the overall properties of FAME.

The CCOO group, constituting a minor fraction of the molecule, exhibits a limited dipole moment and minimal capacity to engage in hydrogen bond formation. Consequently, slight variations in the δP and δH values are observable, such as in the comparison between methyl caprylate and methyl linoleate. However, an exception arises with ricinoleate, which contains a hydroxyl group at C-12, resulting in notably higher δP and δH values compared to other esters.

Table 2. Hansen parameters and the corresponding Teas parameters.

Compound Name	Hansen Parameters			Teas Parameters		
	δd	δp	δh	Fd	Fp	Fh
Methyl Canolate	14.8	2.7	4.5	67.3	12.3	20.5
Methyl Caprate (Methyl decanoate)	15.9	2.4	5.7	66.3	10.0	23.8
Methyl Caproate (Methyl hexanoate)	16.0	4.3	5.8	61.1	16.6	22.3
Methyl Caprylate (Octanoate)	15.4	2.7	5.9	64.2	11.3	24.6
Methyl Cocinate	16.0	1.8	4.7	71.1	8.0	20.9
Methyl Laurate (Methyl Dodecanoate)	16.0	2.1	5.2	68.7	9.0	22.3
Methyl Linoleate	16.2	1.6	3.9	74.7	7.4	18.0
Methyl Linolenate	16.2	1.7	4.2	73.3	7.7	19.0
Methyl Myristate (Methyl tetradecanoate)	16.0	1.9	4.2	72.4	8.6	19.0
Methyl Oleate (Methyl (Z)-9-Octadecenoate)	16.1	1.5	3.5	76.3	7.1	16.6
Methyl Palmitate	16.0	1.6	3.6	75.5	7.5	17.0
Methyl Ricinoleate	16.4	3.5	9.3	56.2	12.0	31.8
Methyl Stearate	15.9	1.4	3.2	77.6	6.8	15.6
Metthyl Soyate	16.1	1.6	3.8	74.9	7.4	17.7
Agnique [®] ME (mix methyl ester)	16.4	3.3	4.7	67.2	13.5	19.3

Table 3 displays the relative energy difference (RED) of FAME shown in Table 2, calculated using white spirit as reference.

Table 3. Hansen parameters and the RED values calculated in relation to white spirit (highlighted in green).

Compound Name	dD	dP	dH	RED
Agnique [®] ME (mix methyl ester)	16.4	3.3	4.7	0.80
Methyl Canolate	14.8	2.7	4.5	0.77
Methyl Caprate (Methyl decanoate)	15.9	2.4	5.7	0.84
Methyl Caproate (Methyl hexanoate)	16	4.3	5.8	1.00
Methyl Caprylate (Octanoate)	15.4	2.7	5.9	0.89
Methyl Cocinate	16	1.8	4.7	0.68
Methyl Laurate (Methyl Dodecanoate)	16	2.1	5.2	0.76
Methyl Linoleate	16.2	1.6	3.9	0.58
Methyl Linolenate	16.2	1.7	4.2	0.62
Methyl Myristate (Methyl tetradecanoate)	16	1.9	4.2	0.62
Methyl Oleate (Methyl (Z)-9-Octadecenoate)	16.1	1.5	3.5	0.51
Methyl Palmitate	16	1.6	3.6	0.53
Methyl Ricinoleate	16.4	3.5	9.3	1.38
Methyl Stearate	16	1.4	3.2	0.46
Metthyl Soyate	16.1	1.6	3.8	0.56
Ligroine	15	0	0	0.23
Mineral spirits (white spirit)	15.8	0.1	0.2	0.00

As the affinity for the miscibility of the two substances decreases, RED numbers increase. RED = 0 signifies that solvent 1 can replace solvent 2; RED < 1 indicates compatibility between the two solvents; and RED > 1 suggests their incompatibility. Methyl Caproate and Methyl Ricinoleate are incompatible with ligroin and white spirit.

Figure 3 plots the tested solvents on the Teas chart. On the same Teas' diagram, the area of solubility for different materials used in cultural heritage applications is reported.

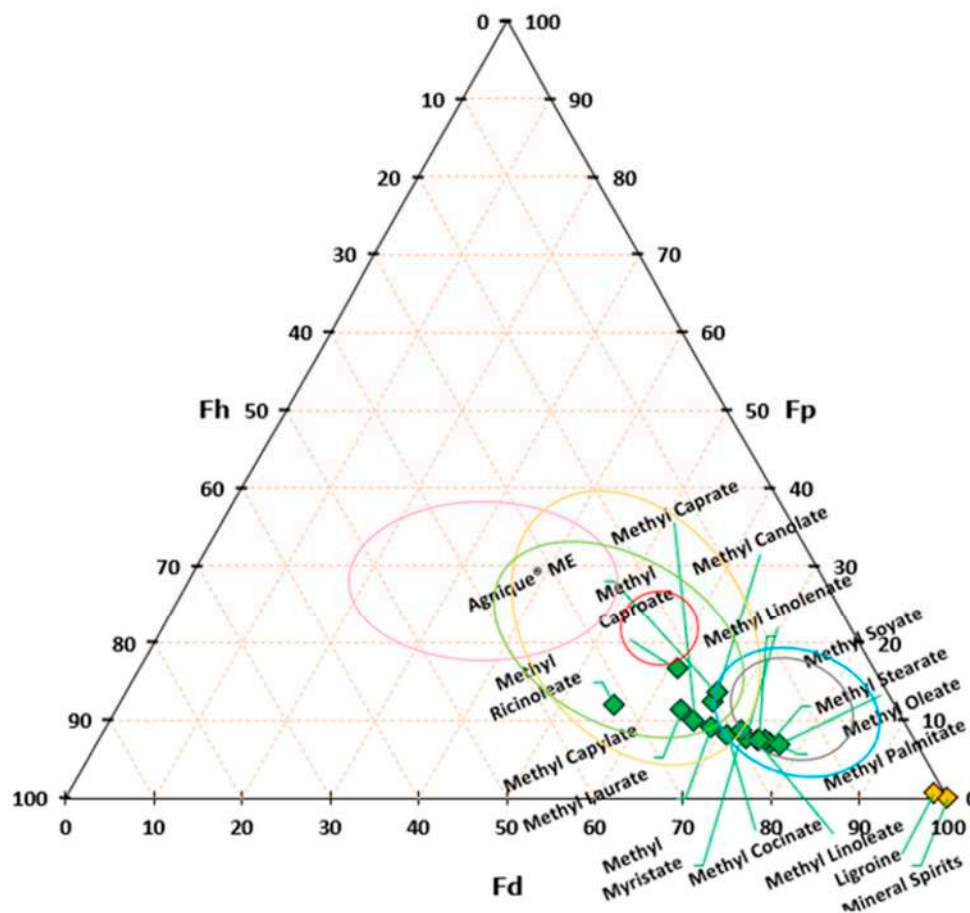


Figure 3. FAME plotted on a Teas chart. Yellow area: synthetic resins; green area: natural resins; grey area: waxes; blue area: oils; red area: polymerized oils; pink area: polysaccharides and proteins.

For the experiment, we selected FAME readily available in the market based on the RED value; a progressively lower affinity toward white spirit was observed (at a value of 0.1). Table 4 lists the FAME used in the experimentation and the name assigned to each gel formulation.

Table 4. Selected FAME used in the experimentation and the gels' names.

ID	Composition
Gel 1	Ligroin/White spirit
Gel 2	Methyl Myristate
Gel 3	Methyl Stearate
Gel 4	Methyl Palmitate
Gel 5	Methyl Oleate
Gel 6	Agnique® ME
Gel 7	Methyl Caprate
Gel 8	Methyl Laurate
Gel 9	poly-hydroxybutyrate (PHB)







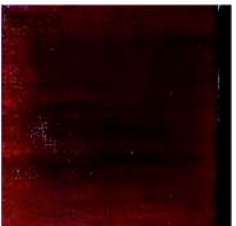



3.2. Visible (Vis) and Ultraviolet (UV) Light Imaging

The observations of the painted canvases allow for the definition of different response to the UV-vis imaging. The untreated canvases revealed visible brush strokes. Under ultraviolet light, the oil-painted canvas exhibited a subtle fluorescence indicative of oil

aging, as discussed by Cairns et al. [34], while canvases painted with acrylic showed no fluorescence [35].

Under visible light, microcrystalline wax displayed an opaque appearance, while Regalrez 1094 varnish exhibited a glossy appearance. In ultraviolet light, neither displayed any fluorescence response, which was attributed to the marker's presence (Fe_3O_4). All cleaning areas exhibited varnish residues. Table 5 presents the images acquired for the oil-based canvases. Gel 3 emerged as the most effective cleaning agent for both microcrystalline wax and Regalrez varnish. It resulted in a level of cleanliness comparable to ligroin for the wax and superior to white spirit for Regalrez 1094.

Table 5. Visible and UV fluorescence images acquired before and after the cleaning test on the canvases prepared with an oil pictorial layer.

	Pictorial Layer without Varnish	Before Cleaning Test		After Cleaning Test	
		Crystalline wax	Regalrez	Crystalline wax	Regalrez
Vis					
UV					

In the evaluation of acrylic canvases (Table 6), all tested gels obtained poorer cleaning outcomes in the designated areas. This outcome might be attributed to a potential interaction between the varnishes and the paint layers, influencing the efficacy of the cleaning process.

Figure 4 shows the percentages of residual black aspect after the cleaning treatment for the various treated areas. The images confirm the result obtained with the macroscopical observations, establishing Gel 3 as the most effective treatment. Based on the percentage of black aspect remaining, the following order for the removal of microcrystalline wax on both oil and acrylic paint layers can be established:

$$\text{Gel 3} > \text{Gel 1} = \text{Gel 2} > \text{Gel 4} = \text{Gel 5} = \text{Gel 6} > \text{Gel 8} > \text{Gel 7} = \text{Gel 9}$$

Regarding the removal of Regalrez 1094 varnish (Figure 5), the following order can be established based on the percentage of remaining black substance after cleaning treatment:





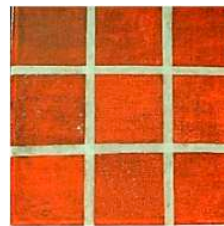



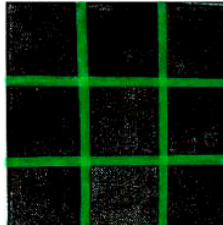
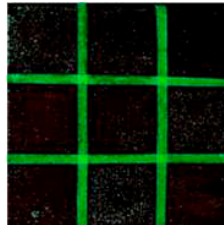
$$\text{Gel 3} = \text{Gel 5} > \text{Gel 7} > \text{Gel 6} = \text{Gel 8} > \text{Gel 1} = \text{Gel 4} > \text{Gel 9}$$

3.3. Digital Microscope Observations

Utilizing optical microscopy, the experiment enabled the evaluation of various gels' cleaning effectiveness and the exploration of potential interactions with the substrate. It is important to highlight that the application of reference solvents in gel formulation resulted in a reduced solvent action compared to their liquid state.

Regarding the oil-painted canvas (Table 7), observations yielded a solvent power ranking for the removal of microcrystalline wax as follows: Gel 3 > Gel 4 > Gel 1 > Gel 2 > Gel 5 = Gel 6 > Gel 7 > Gel 8 > Gel 9.

Table 6. Visible and UV fluorescence images acquired before and after the cleaning test on the canvases prepared with an acrylic pictorial layer.

	Pictorial Layer without Varnish	Before Cleaning Test		After Cleaning Test	
		Crystalline wax	Regalrez	Crystalline wax	Regalrez
Vis					
UV					

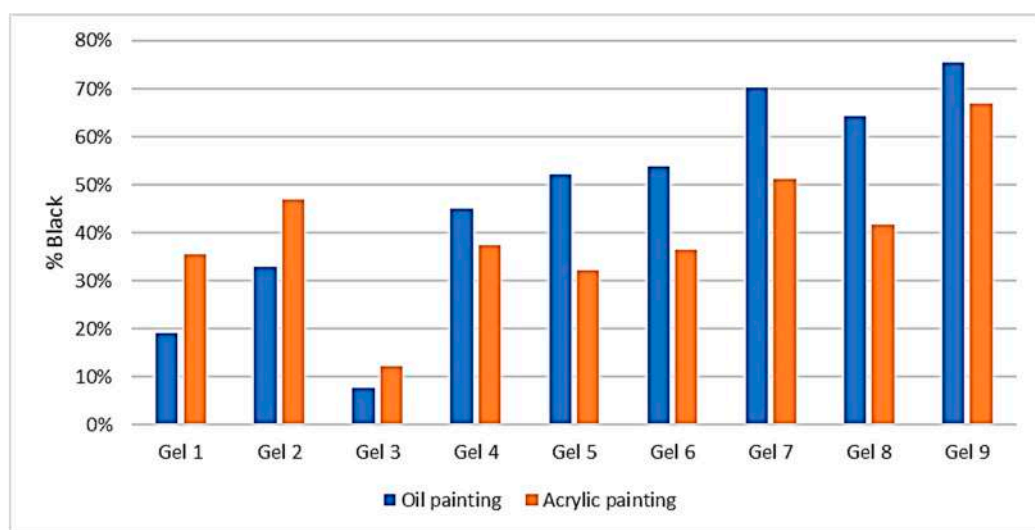


Figure 4. Histograms of the residual black aspect (%) for microcrystalline wax.

Regarding the acrylic canvases coated with Regalrez 1094 varnish, the established order is as follows:

Gel 3 > Gel 5 > Gel 6 > Gel 7 = Gel 8 > Gel 2 = Gel 4 > Gel 1 > Gel 9

The application of all the different FAME gels on acrylic surfaces unveiled distinct interaction with the substrate. Conversely, no discernible interactions were noted on the oil-painted surface.

3.4. Spectrocolorimetric Analysis

To evaluate the cleaning effectiveness, spectrocolorimetric analyses were carried out before and after the cleaning test to determine whether the color of the surface had returned to the color measured before cleaning. Figure 6 reports the total chromatic variation (ΔE). The areas represent zones that are cleaned, partially cleaned, or marked by varnish residues; consequently, the standard deviation associated to the measurements is high and thus not reported.

For the canvases coated with acrylic layers (Table 8) and treated with microcrystalline wax, Gel 3 demonstrated the most effective removal of the coating, while Gel 9 showed no efficacy. Visible residues were observed with Gel 5, Gel 1, Gel 6, and Gel 2, whereas Gel 8 and Gel 7 exhibited partial residue removal.

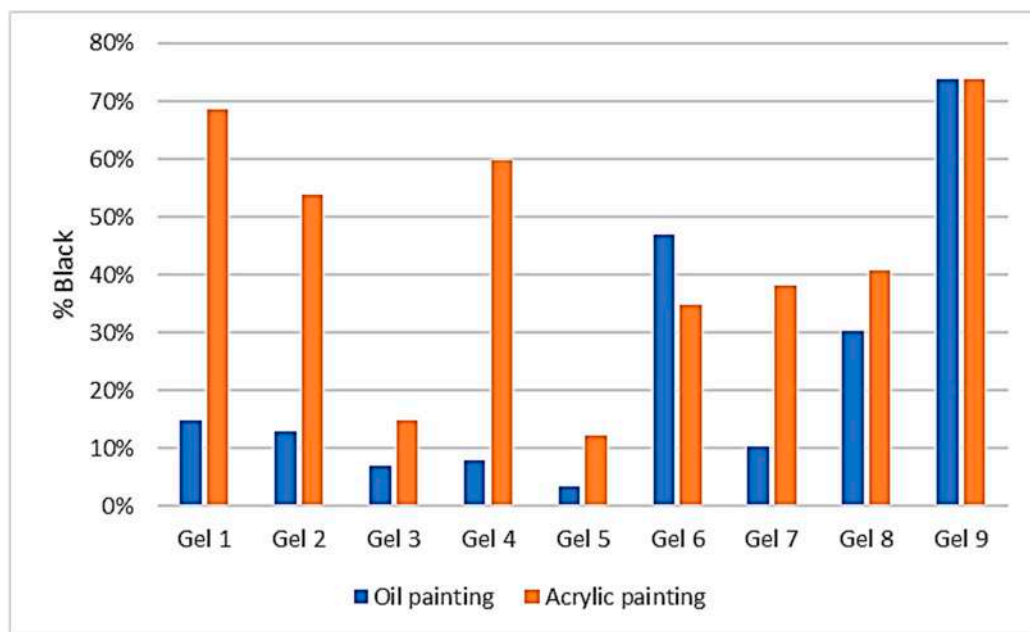


Figure 5. Histograms of the residual black aspect (%) for Regalrez 1094 varnish.

Table 7. Microscopic images acquired after the cleaning test on the oil-prepared canvases.

	Oil Painting			
	Microcrystalline wax		Regalrez 1094 varnish	
	Vis	UV	Vis	UV
Gel 1				
Gel 2				

Table 7. Cont.


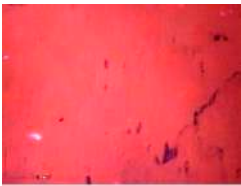

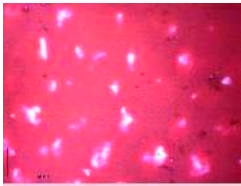

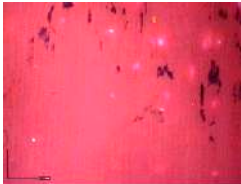
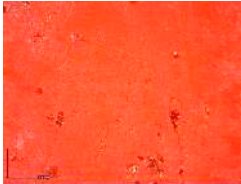
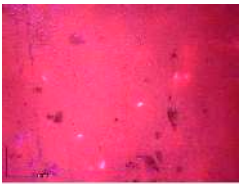

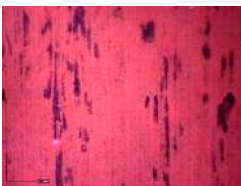

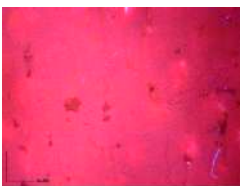




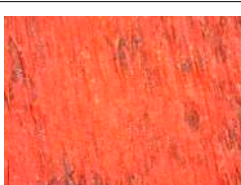
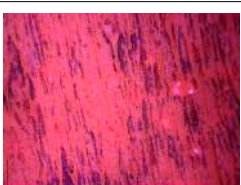
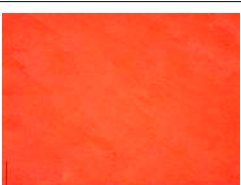
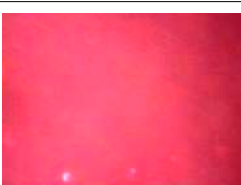
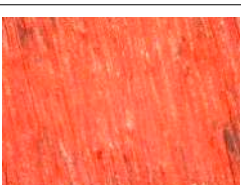
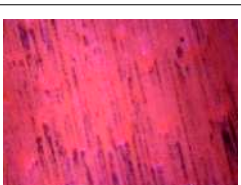
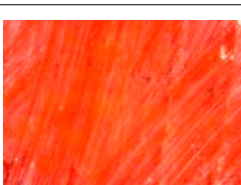


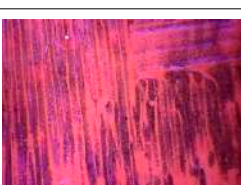
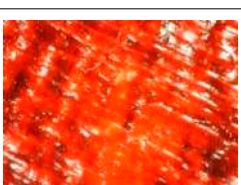
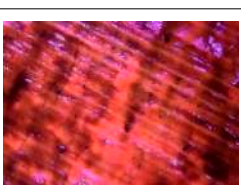
	Oil Painting			
Gel 3				
Gel 4				
Gel 5				
Gel 6				
Gel 7				
Gel 8				
Gel 9				

Table 8. Microscopic images acquired after the cleaning test on the acrylic-prepared canvases.

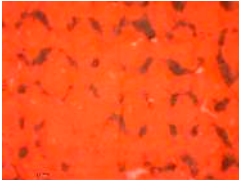
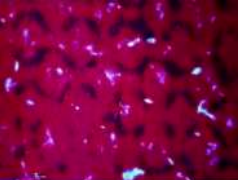

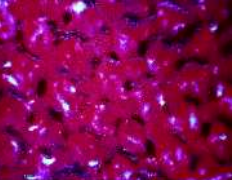
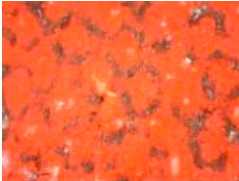
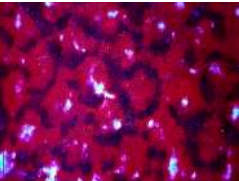

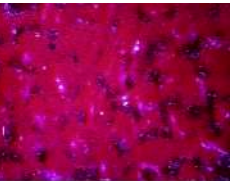

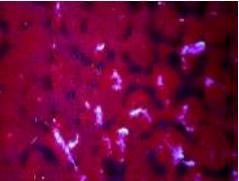

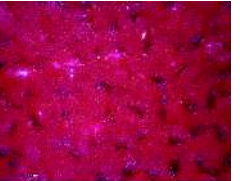

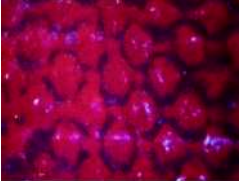

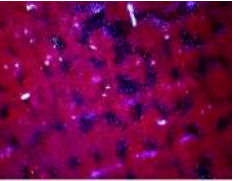

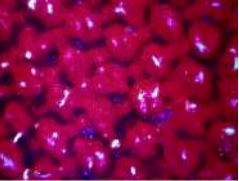

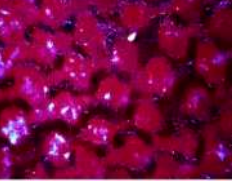
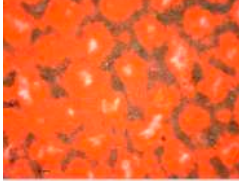
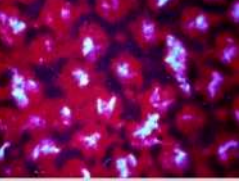

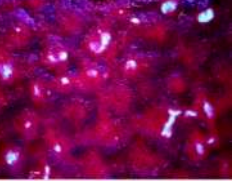
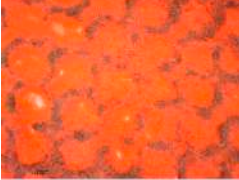
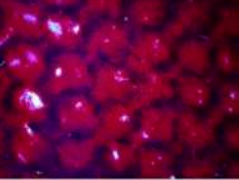

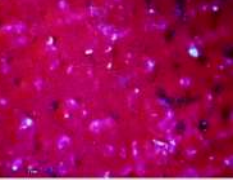

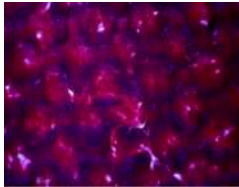
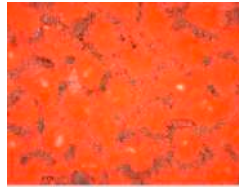
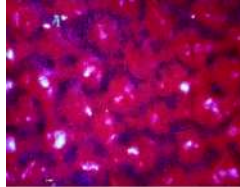
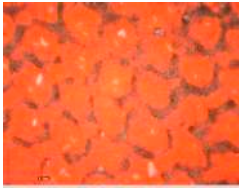
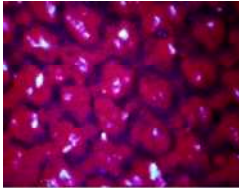
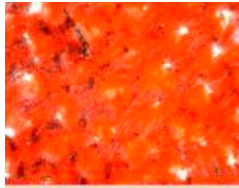
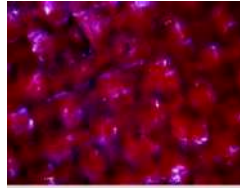
		Acrylic Painting			
		Microcrystalline wax		Regalrez 1094 varnish	
		Vis	UV	Vis	UV
Gel 1					
Gel 2					
Gel 3					
Gel 4					
Gel 5					
Gel 6					
Gel 7					

Table 8. Cont.

		Acrylic Painting			
Gel 8					
Gel 9					

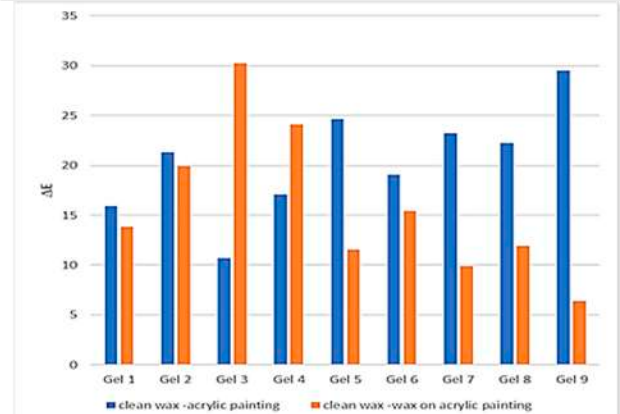
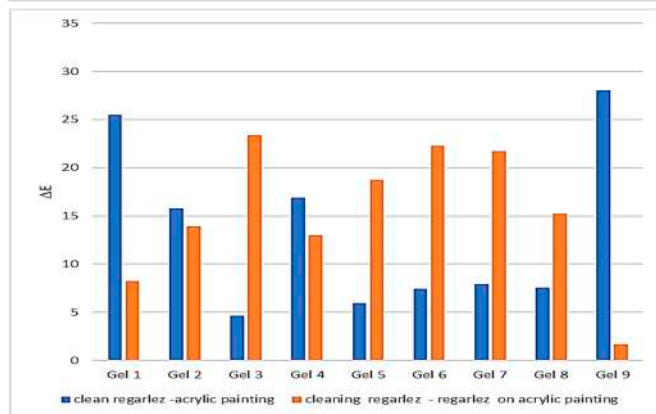
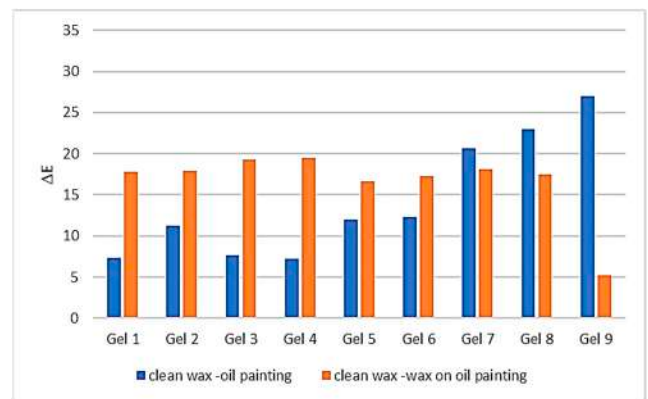
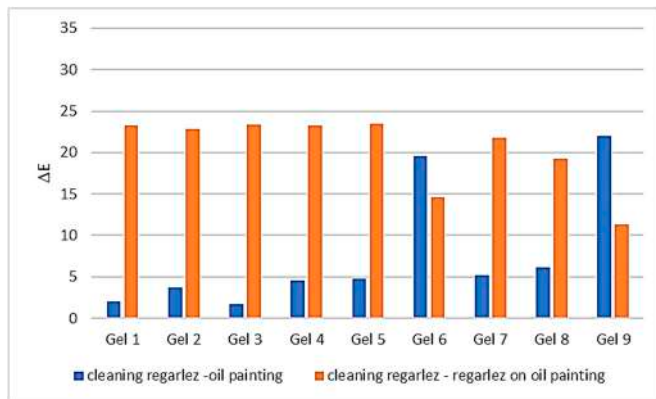


Figure 6. Histograms showing the results of total colour variation calculation.

The data highlight that for all cleaning systems used, the colour values of the cleaned surface and the painted surface differ. This difference is significant for canvases painted with acrylic; for oil-painted canvases, however, some cleaning systems achieve ΔE values < 5 , making the differences imperceptible to the human eye [36].

For the acrylic-painted and wax-finished canvas, the area treated with Gel 3 presents the greatest disparity relative to the coated canvas and the smallest difference compared to the canvas surface covered only with the acrylic paint layer.

The ratio between the ΔE , representing the difference between the dirty surface and the surface of canvas with only the acrylic varnish on ΔE of the surface cleaned with Gel 3 of the acrylic-painted canvas coated with microcrystalline wax, is 0.4. Below is this ratio calculated for other gels:

$$\text{Gel 3 (v = 0.4)} > \text{Gel 4 (v = 0.7)} < \text{Gel 1} = \text{Gel 2 (v = 1.1)} < \text{Gel 6 (v = 1.2)} < \\ \text{Gel 8 (v = 1.8)} < \text{Gel 5 (v = 2.1)} = \text{Gel 7 (v = 2.3)} < \text{Gel 9 (v = 4.6)}.$$

The lower this ratio, the more the surface appearance is akin to that of the original painted canvas. The most effective cleaning treatments were executed using Methyl Stearate and Methyl Palmitate FAME, which provided superior results compared to ligroin gel.

Upon examining the oil-painted canvas (also coated with microcrystalline wax) and analysing the data through the same ratio, the following order can be defined: Gel 1 = Gel 3 = Gel 4 (v = 0.4) < Gel 2 (v = 0.6) < Gel 5 = Gel 6 (v = 0.7) < Gel 7 (v = 1.1) < Gel 8 (v = 1.3) < Gel 9 (v = 5.3). These data facilitate the superior cleaning capability of all the experimental systems for the oil-painted canvas relative to the same treatment performed on the acrylic-painted canvas. Considering the results obtained in the cleaning of the Regalrez 1094 varnish covering the acrylic paint layer, the relationship between the chromatic variations of the cleaned area with respect to the painted canvas and the chromatic variations relative to the varnish layer defines the following cleaning order:

$$\text{Gel 3} = \text{Gel 5} = \text{Gel 6} = \text{Gel 7} = \text{Gel 8 (0.2 < v < 0.5)} < \text{Gel 2} = \text{Gel 4 (v = 1.1)} < \text{Gel 1 (v = 3.1)} < \text{Gel 9 (v = 16.6)}.$$

A greater cleaning effect of the various FAME tested was observed following application of the Regalrez 1094 varnish over the oil paint layer. All the tested Gels present a v ratio < 0.3, apart from Gel 6 and Gel 9.

3.5. FTIR-ATR

The main peaks in the FTIR spectra of the painting sample surfaces are listed in Table 9. C–H stretching vibrations of the –CH₃ and –CH₂ groups were located in the 2950–2800 cm^{−1} area. The C=O double bond stretching vibration of carbonyl groups was present around 1745 cm^{−1}. The peaks in the 1470–1200 cm^{−1} area are associated with the CH bending of CH₂ and CH₃. Due to CH₂ rocking vibration and C–O ester group stretching vibration, the fingerprint region was located between 1250 and 700 cm^{−1}.

Table 9. IR assignment of the peaks collected on the painting material (unaged and aged).

Unaged Acrylic Painting Surface	Unaged Oil Painting Surface	Aged Acrylic Painting Surface	Aged Oil Painting Surface	Assignment
	3010		2923	CH ₃ stretch
	2897		2852	CH ₂ stretch
1712	1746	1735	1739	C=O
	1655		1652	C=C
1474	1408	1403	1408	CH ₃ Asymmetric bend
1240		1227		C–O ester bond
1170		1155		CCH (C=C)
1150		1120		C–O Ester bond
	1021	1013	1021	C–O Ester bond
	872	870	872	
		753		C–H2
	710	711	710	C=C–H (cis) bend

The FTIR spectra (Figure 7) acquired from Methyl caprate, Methyl laurate, Methyl myristate, and Methyl oleate show the same characteristic peaks at 2921, 2852, 1458, 1434, 1358, 1239, 1195, 1169, 1009, 719, 711, and 700 cm^{−1}. Similarly, the Methyl palmitate, Methyl stearate, and Agnique ME have peaks at 2951, 2914, and 2847 cm^{−1}, albeit with different

intensity to the first, while in the Methyl stearate the peak at 1741 cm^{-1} was not present. Methyl stearate and Agnique ME have peaks at $1471, 1462, 1343, 1279, 1241, 1446, 1109, 1059, 1023, 964, 839, 731,$ and 718 cm^{-1} . Methyl palmitate was instead characterized by numerous peaks in the region between 1500 and 1000 cm^{-1} ; specifically, the peaks were at $1472, 1462, 1434, 1381, 1309, 1286, 1264, 1241, 1219, 1196, 1167, 1099, 883, 729,$ and 719 cm^{-1} .

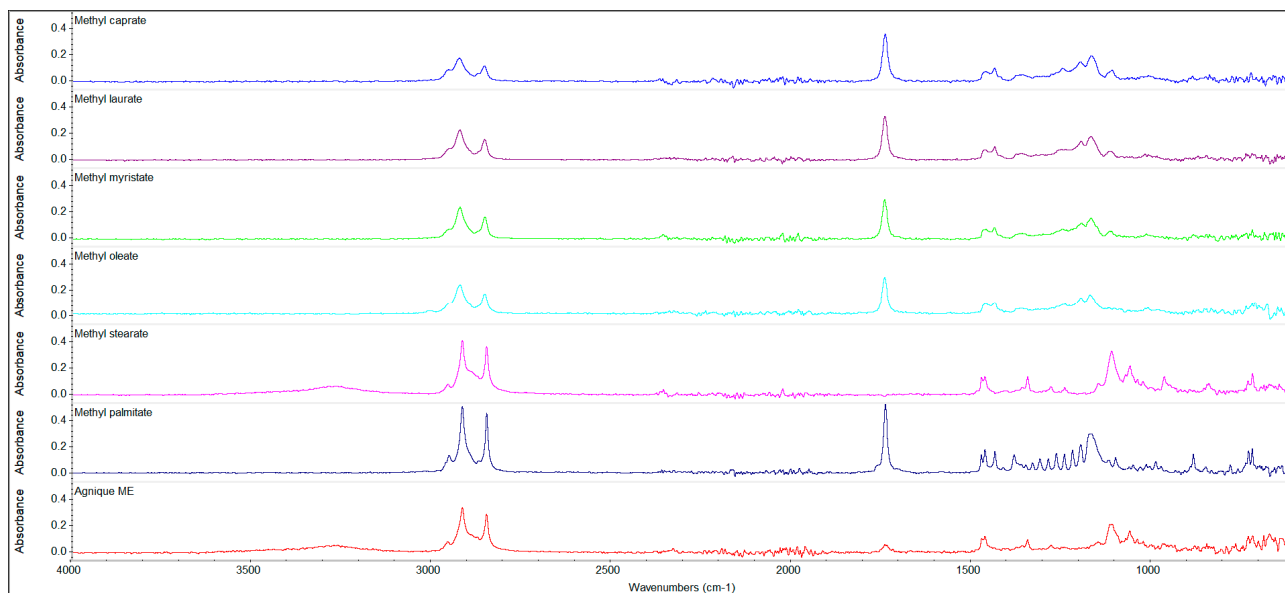
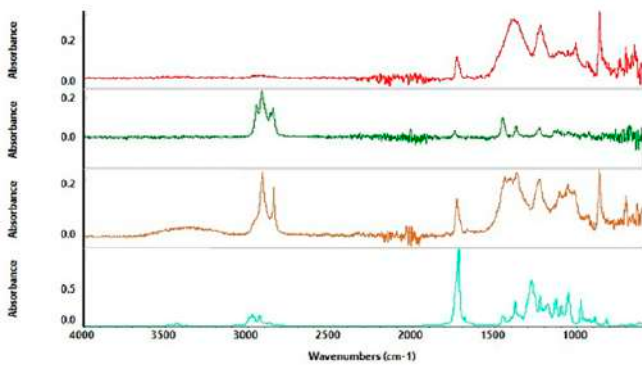


Figure 7. All the spectra collected for each FAME used in the experimentation.

Regarding the coatings, some variation in the IR spectrum after the aging process was observed only for Regalrez 1094. In particular, the aged Regalrez spectrum is characterized by increasing absorption of the hydroxyl region between 3650 and 3050 cm^{-1} , suggesting the formation of new O–H bonds. Furthermore, a new absorption band appears at 1712 cm^{-1} with the appearance of new C=O bonds. Additionally, there is a slight increase in absorption at 1200 cm^{-1} , indicating the appearance of C–O bonds. These structural changes suggest that upon irradiation, the hydrogenated hydrocarbon resin undergoes photo-oxidation with the generation of new oxidation products. There is an observable decrease in absorption for the C–H stretching and bending regions, $3000\text{--}2750\text{ cm}^{-1}$ and $1500\text{--}1400\text{ cm}^{-1}$, respectively. It is uncertain exactly why these bands decrease so much in intensity, but it could be related to photo-oxidation of the material [37].

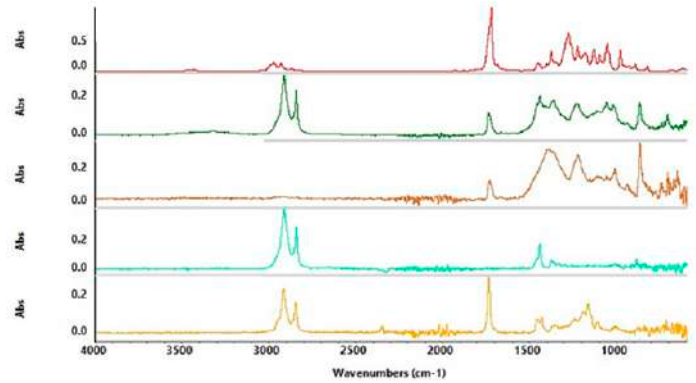
To define the presence of residue of FAME gels, spectra were acquired on the cleaned canvases; on the coated canvases, on the canvases after the cleaning treatment, and on the spectra of all the solvents and the polymer used for the formulation of the gels (PHB) (Figures 8–11).

Considering the overlap of the same peaks relative to functional groups present in all the substances, to define FAME gel residues, more consideration was given to the “Fingerprint” region. This region represents peculiar characteristics of the substance, while the other regions of the spectra are related to functional groups that may be present in different kinds of molecules; in this study, this was the case for the non-polar coating and the FAME. To evaluate the presence of the polymer PHB, the peaks at 1280 cm^{-1} and 1057 cm^{-1} were searched in the spectrum acquired on the canvas after the cleaning treatment. For the FAME, specific peaks were taken into consideration.



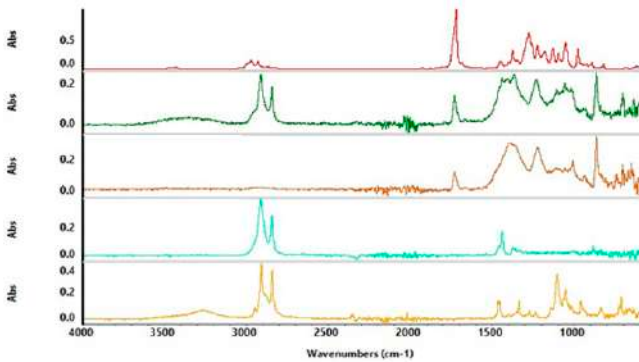
Gel 1

Acrylic canvas in red. White spirit in green. Residue of Gel 1 (White spirit + PHB) in brown, PHB spectrum in blue.



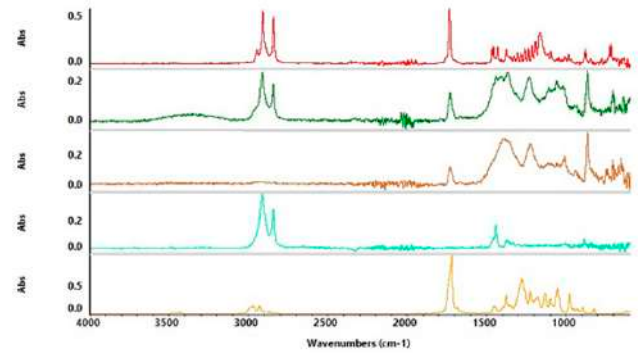
Gel 2

Acrylic canvas in brown, Acrylic coated with Regalrez 1094 (RG) in blue, residue after cleaning in green, PHB spectrum in red, Methyl myristate in yellow.



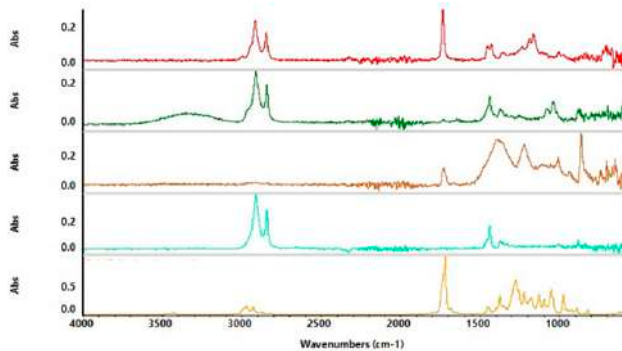
Gel 3

PHB only in red, residue after cleaning in green, acrylic canvas in brown, acrylic + RG in blue, Methyl stearate in yellow.



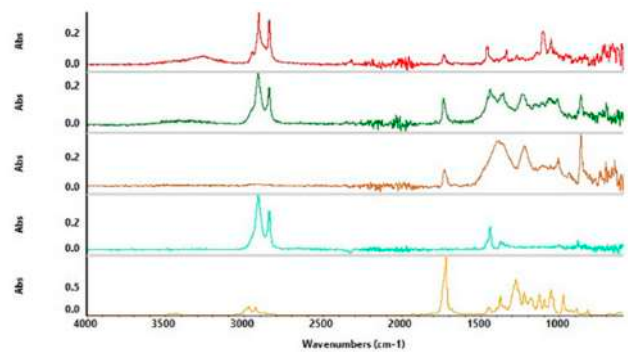
Gel 4

Methyl palmitate in red, residue in green, acrylic canvas in brown, acrylic + RG in blue, PHB only in yellow.



Gel 5

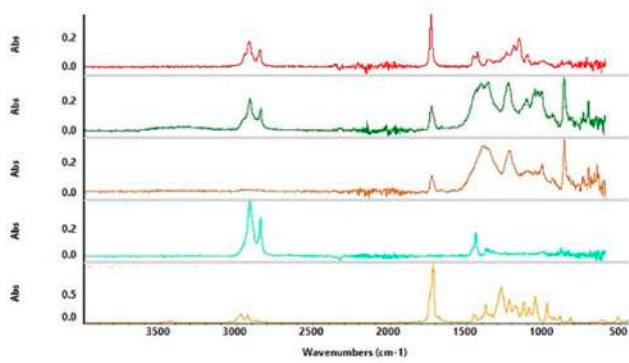
Methyl oleate in red, residue after cleaning in green, acrylic canvas in brown, acrylic + RG in blue, PHB only in yellow.



Gel 6

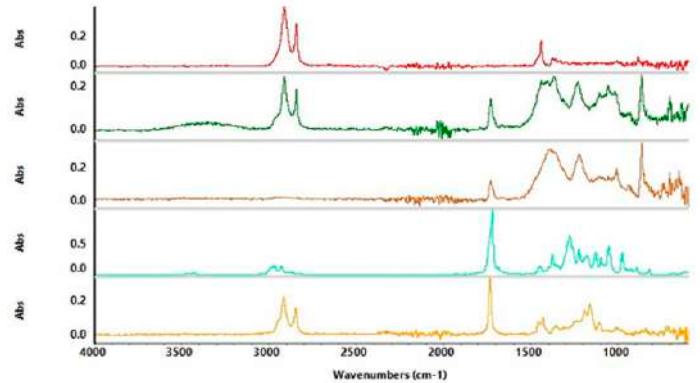
Agnique® ME in red, residue after cleaning in green, acrylic canvas in brown, acrylic + RG in blue, PHB only in yellow.

Figure 8. Cont.



Gel 7

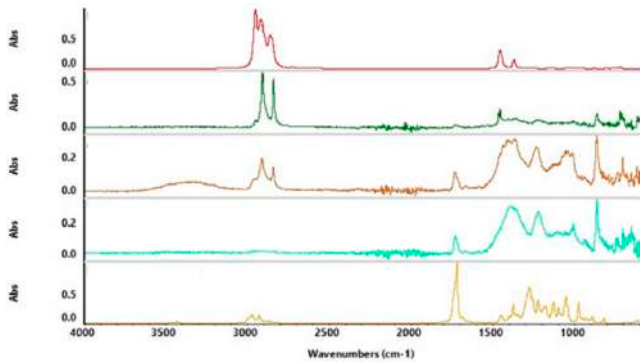
Methyl caprate in red, residue after cleaning in green, acrylic canvas in brown, acrylic +RG in blue, PHB only in yellow.



Gel 8

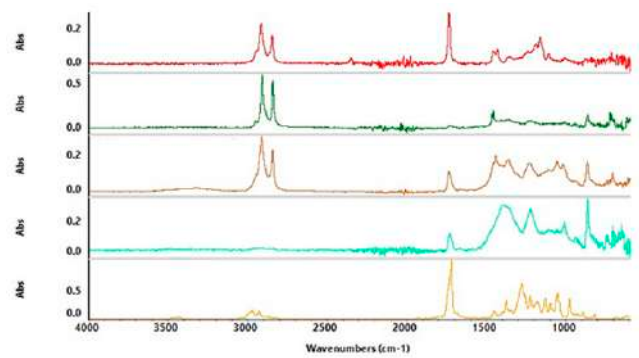
Acrylic + RG in red, residue after cleaning in green, acrylic canvas in brown, PHB only in blue, Methyl laurate in yellow.

Figure 8. All the FTIR spectra acquired for the acrylic painting coated with Regalrez 1094 varnish.



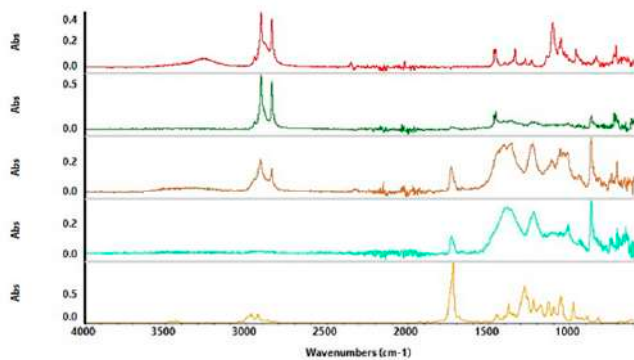
Gel 1

Ligroin in red, acrylic + microcrystalline wax in green, residue after cleaning in brown, acrylic canvas in blue, PHB only in yellow.



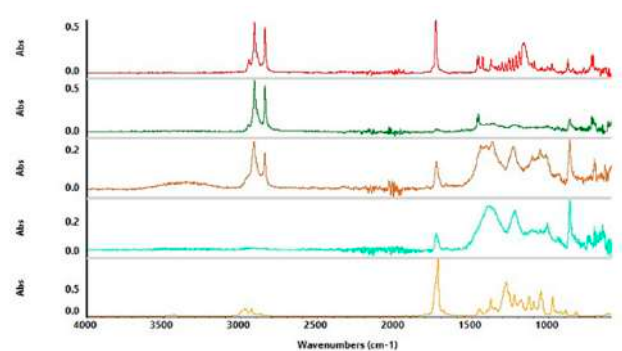
Gel 2

Methyl myristate in red, acrylic + wax in green, residue after cleaning in brown, acrylic canvas in blue, PHB only in yellow.



Gel 3

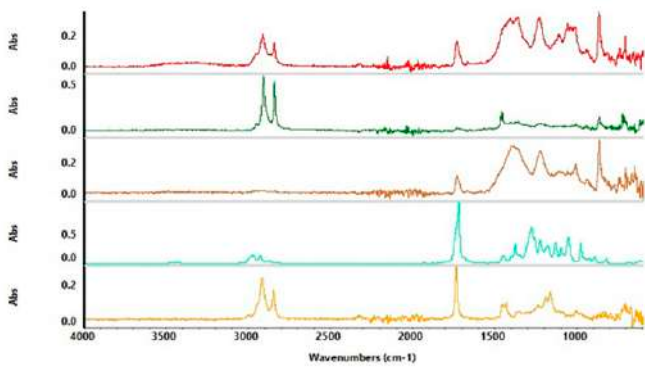
Methyl stearate in red, acrylic + wax in green, residue after cleaning in brown, acrylic canvas in blue, PHB only in yellow.



Gel 4

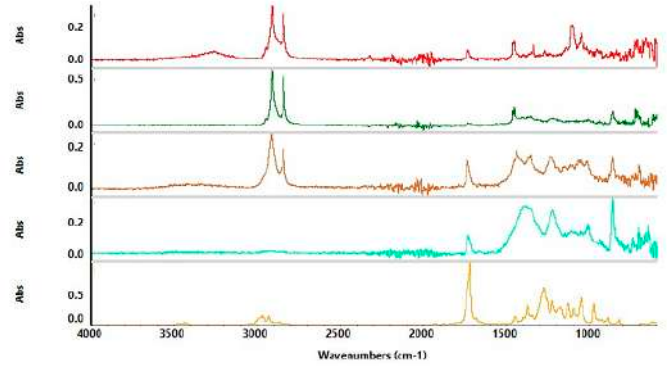
Methyl palmitate in red, acrylic + wax in green, residue after cleaning in brown, acrylic canvas in blue, PHB only in yellow.

Figure 9. Cont.



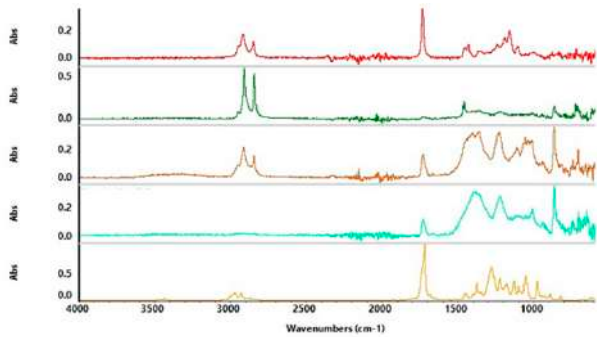
Gel 5

Residue after cleaning in red, acrylic + wax in green, acrylic canvas in brown, PHB only in blue, Methyl oleate in yellow.



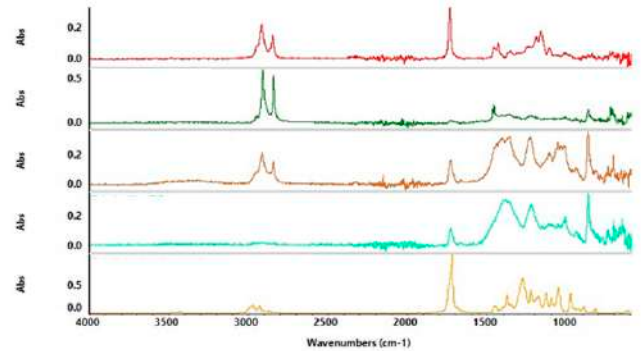
Gel 6

Agnique® ME in red, acrylic + wax in green, residue after cleaning in brown, acrylic canvas in blue, PHB only in yellow.



Gel 7

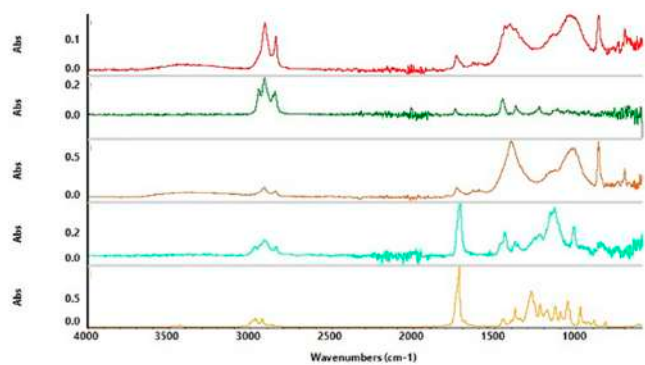
Methyl caprate in red, acrylic + wax in green, residue after cleaning in brown, acrylic canvas in blue, PHB only in yellow.



Gel 8

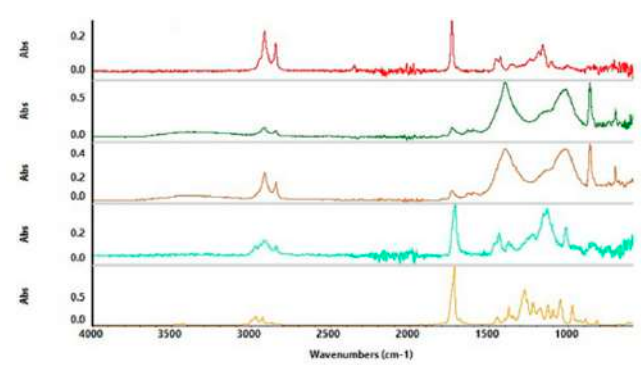
Methyl laurate in red, acrylic + wax in green, residue after cleaning in brown, acrylic canvas in blue, PHB only in yellow.

Figure 9. All the FTIR spectra acquired for the acrylic painting coated with microcrystalline wax.



Gel 1

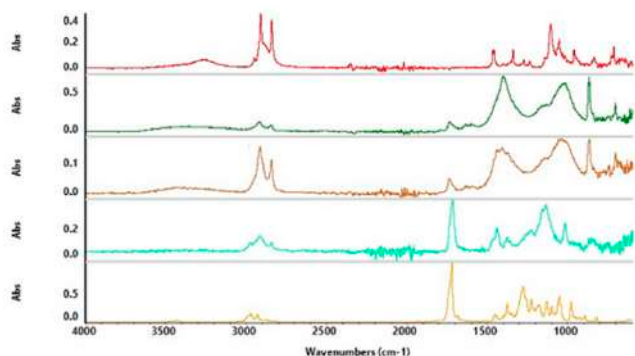
Oil canvas in brow, oil + RG in blues, residue after cleaning in red, white spirit spectra in green, PHB only in yellow.



Gel 2

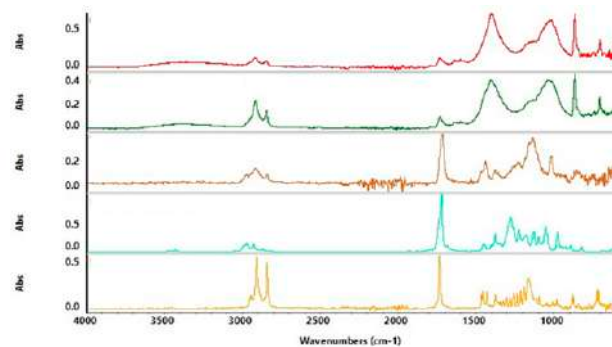
Methyl myristate in red, oil canvas green, residue after cleaning in brown, oil + RG in blue, PHB only in yellow.

Figure 10. Cont.



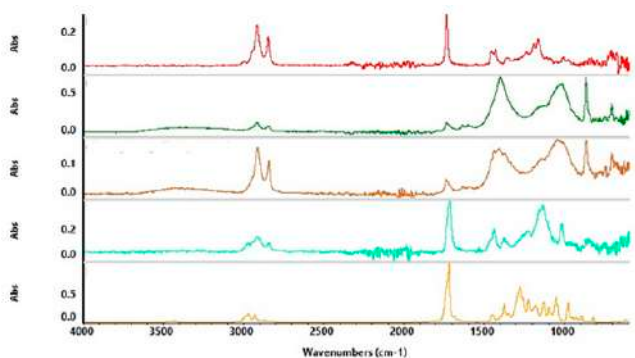
Gel 3

Methyl stearate in red, oil canvas in green, residue after cleaning in brown, oil + RG in blue, PHB only in yellow.



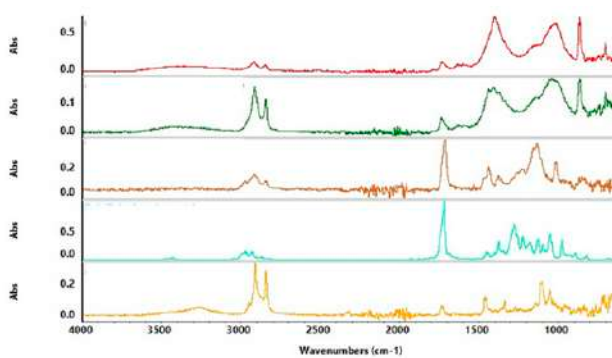
Gel 4

Oil canvas in red, residue after cleaning in green, oil + RG in brown, PHB only in blue, Methyl palmitate in yellow.



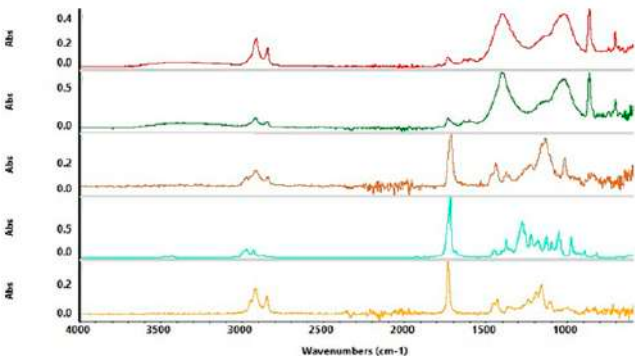
Gel 5

Methyl oleate in red, olio canvas in green, residue after cleaning in brown, oil + RG in blue, PHB in yellow.



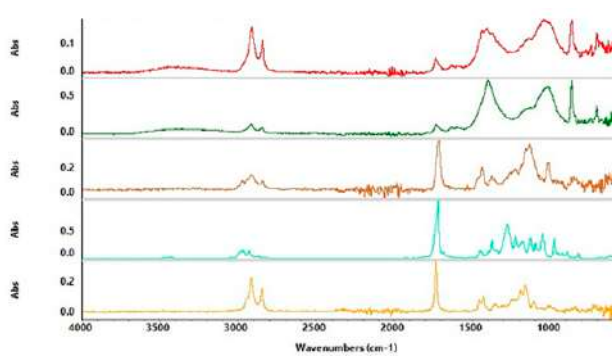
Gel 6

Oil canvas in red, residue after cleaning in green, oil + RG in brown, PHB only in blue, Agnique® ME in yellow.



Gel 7

Residue after cleaning in red, oil canvas in green, oil + RG in brown, PHB in blue, Methyl caprate in yellow.

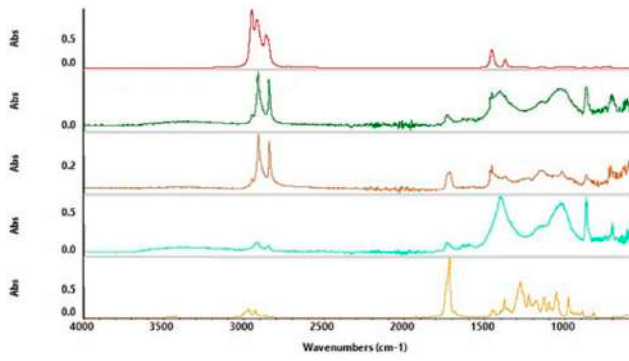


Gel 8

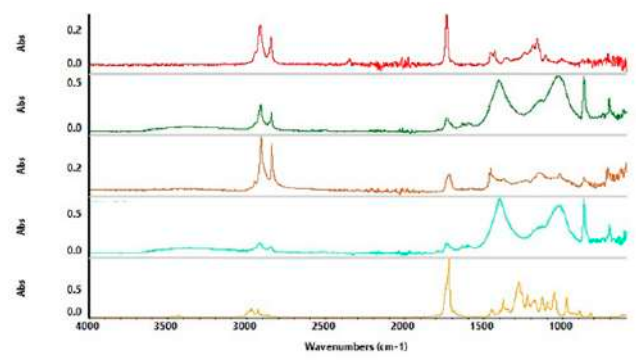
Residue after cleaning in red, oil canvas in green, oil + RG in brown, PHB in blue, Methyl laurate in yellow.

Figure 10. All the FTIR spectra acquired for the oil painting coated with Regalrez 1094 varnish.

For example, the spectra acquired on the canvas prepared with an acrylic layer coated with Regalrez 1094 varnish and treated with Gel 3 show no presence of the PHB peaks ($1280\text{--}1057\text{ cm}^{-1}$) nor the FAME (Methyl stearate, in this case) peak at 1239 cm^{-1} . The peaks at $2917\text{--}2848\text{ cm}^{-1}$ in the spectrum collected after the cleaning treatment, were attributed to the presence of some residue of Regalrez 1094 on the painted canvas.

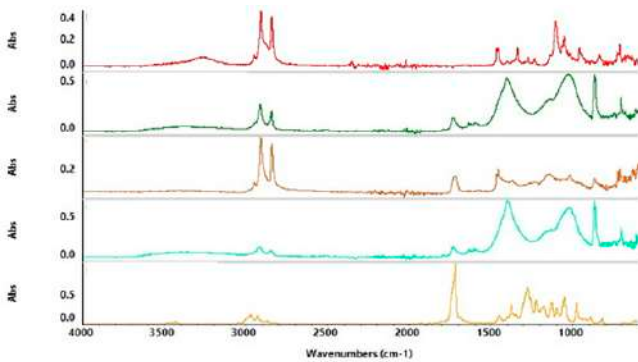


Gel 1

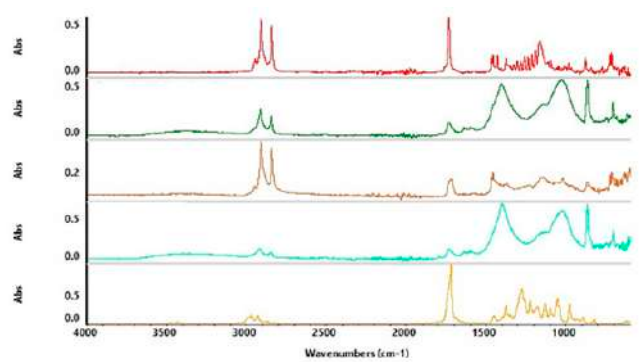


Gel 2

Ligroin in red, residue after cleaning in green, oil + wax in Methyl myristate in red, residue after cleaning in green, oil + wax in brown, oil canvas in blue, PHB only in yellow.

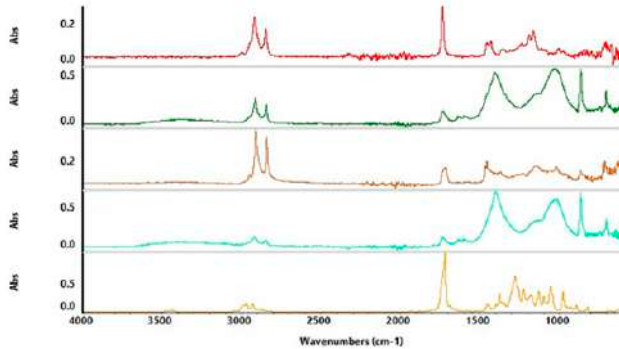


Gel 3

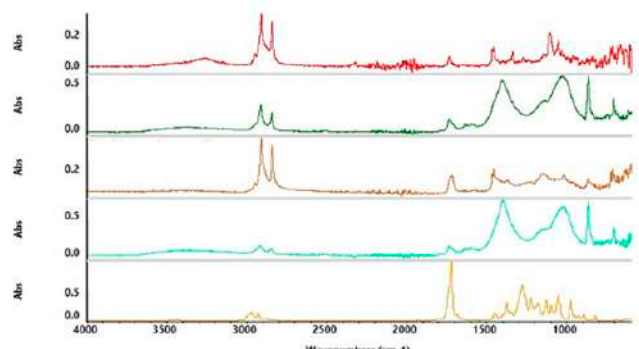


Gel 4

Methyl stearate in red, residue after cleaning in green, oil + wax in brown, oil canvas in blue, PHB only in yellow. Methyl palmitate in red, residue after cleaning in green, oil + wax in brown, oil canvas in blue, PHB only in yellow.



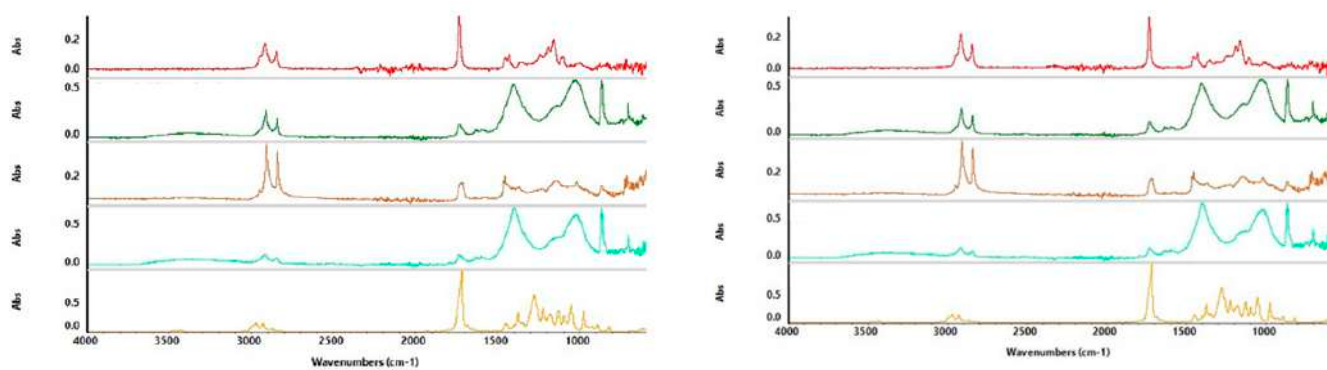
Gel 5



Gel 6

Methyl oleate in red, residue after cleaning in green, oil + wax in brown, oil canvas in blue, PHB only in yellow. Agnique[®] ME in red, residue after cleaning in green, oil + wax in brown, oil canvas in blue, PHB only in yellow.

Figure 11. Cont.



Gel 7

Gel 8

Methyl caprate in red, residue after cleaning in green, oil + wax in brown, oil canvas in blue, PHB only in yellow. Methyl laurate in red, residue after cleaning in green, oil + wax in brown, oil canvas in blue, PHB only in yellow.

Figure 11. All the FTIR spectra acquired for the oil painting coated with microcrystalline wax.

The collected spectra after the cleaning are characterized by the presence of some residues of the Regalrez 1094 varnish or microcrystalline wax on the surface, defined by the following peaks: $2916\text{--}2848\text{ cm}^{-1}$ for the microcrystalline wax and $2917\text{--}2848\text{ cm}^{-1}$ for the Regalrez 1094 varnish.

However, for all the different cleaning treatments, no peaks related to gel or FAME were found.

3.6. Scanning Electron Microscopy (SEM) Analysis

The diverse outcomes obtained in the cleaning tests can be justified by the morphology of the painted surfaces. Below, SEM analyses of painted canvases subjected to aging treatment are presented, aiming to simulate a condition as close as possible to the characteristic surfaces of cultural heritage.

The SEM images obtained (Figure 12) through backscattered electrons reveal a high porosity of the surface painted with acrylic. This result is attributed to the ageing-induced shrinkage phenomena compared to oil-painted canvas. This result allows us to hypothesize heightened interaction between the acrylic-painted layer and the applied varnishes, leading to increased difficulty in cleaning.

Surface of Aged Acrylic Canvas

Surface of Aged Oil Canvas

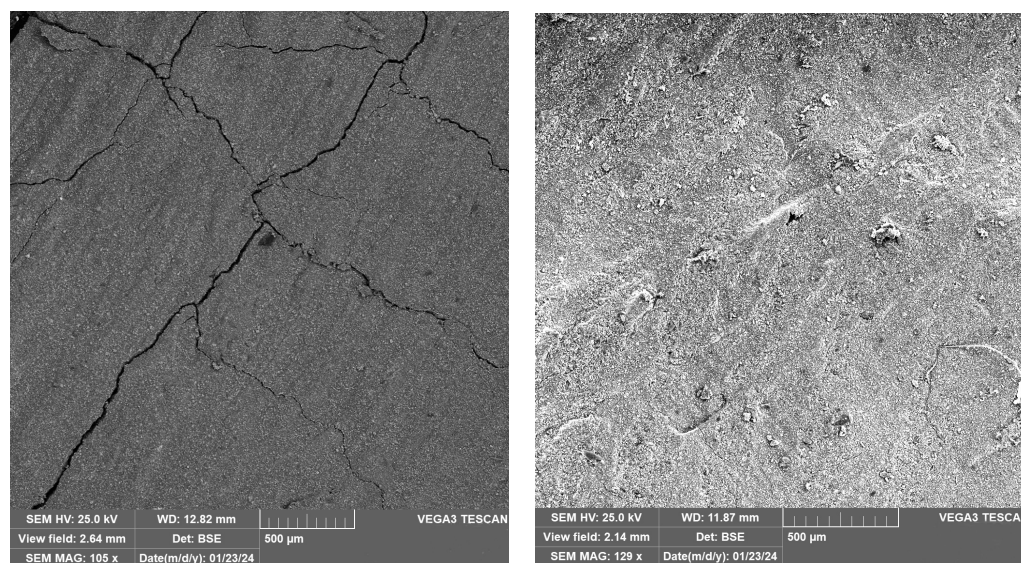


Figure 12. SEM images acquired on the canvases before the application of the non-polar coatings.

4. Discussion

Solubility and optical characteristics are often crucial considerations for conservators, and an intriguing correlation between the two emerges through the study of cleaning. The observation of morphological variations induced during cleaning allows for an understanding of the effectiveness of new green solvents in applications similar to real cases. The data collected from various analytical techniques confirm the predictions developed using RED calculations in the Hansen diagram, compared to what is expected from the TEAS diagram.

All tested FAME can be utilized to solubilize two of the most commonly used low- and non-polar substances in the cultural heritage sector. The best results were obtained from FAME characterized by carbon chain lengths ranging from C16 to C18, both in the removal of microcrystalline wax and Regarlez paint applied on canvas painted with acrylic and oil. The FAME were applied in gel form through a single step with a contact time of 5 min. This method was chosen to avoid potential interactions with the support and to compare the effectiveness of the different tested FAME. A second application, considering the different efficiency of the tested FAME, would have led to total cleaning in some areas, with the possibility of interacting with the surface, thus not allowing a real comparison. Optical microscopy images confirmed the hypotheses developed through macroscopic observations, highlighting greater interaction between the paints and the canvas painted with acrylic. This result is attributed to the aging process, which causes acrylic to retract more compared to the oil-painted layer, as observed in SEM images. Microscopy observations correlated with spectrophotometric analyses show that with an increase in non-polar carbon chain length, solubility typically increases. However, greater efficiency was achieved with FAME characterized by saturated chains compared to FAME characterized by structures of the allylic and bis-allylic methylene groups.

The overall analysis data allowed us to assess the efficacy of the gel formulation in both removal and interaction with the underlying canvas, evaluating the presence of surface residues through optical microscopy and FTIR spectra, enabling us to achieve the objectives set in the introduction. Different gels were defined for the various canvas compositions, highlighting the extensive customization possibilities of the gel based on specific case needs. Further studies are necessary to evaluate the stability of gel-FAME-emulsifier systems, for example, through aging cycles.

In synthesis, concerning the canvas painted with oil colour and coated with microcrystalline wax, the optimal results, following various analyses, were achieved using Gel 3 (the best surface cleaning seems to have been obtained with Gels 1, 3, and 4 from imaging observation; with optical microscopy observation, the best cleaning results were obtained with Gels 1, 3, 4, and partially with Gel 5; colorimetry revealed a ΔE value of 1.36 for Gel 3). For the canvas painted with oil and coated with Regalrez resin, the best outcomes were obtained with Gel 1, Gel 3, Gel 7, and Gel 4 (the best cleaning appears to be given by Gels 1, 2, 3, 4, 5, and 7 from imaging observation; with optical microscopy observation, the best results were provided by Gels 1 and 7; colorimetry showed the lowest values for Gels 1, 4, and 2).

For the canvas painted with acrylic and coated with microcrystalline wax, the most favorable results were obtained using Gel 3 (imaging showed cleaning results with Gels 1, 3, 5, and 6; optical microscopy observation indicated Gel 3, and partially Gel 5; colorimetry showed a lower ratio value for Gel 3 and Gel 5). Regarding the canvas painted with acrylic and coated with Regalrez resin, the optimal results were achieved with Gel 3 and Gel 5 (imaging demonstrated better cleaning results with Gels 3, and partially scarce results with Gel 5 and 2; optical microscopy observation confirmed those results).

5. Conclusions

The present study enabled us to evaluate the possible use of FAME as substitutes of more toxic solvents used in the cleaning of non-polar or low polar substances and assess their solubility power toward those materials. The tests carried out highlighted the

possibility of using FAME through a gel formulation and the customizable characteristics of FAME based on the specific material properties.

Due to their minimal volatile organic compound (VOC) emissions and non-toxic nature, FAME Gels represent suitable candidates to replace organic solvents used in conservation practices, thereby helping to safeguard the health of operators. From the cleaning tests conducted, FAME were able to solubilize both microcrystalline wax and Regalrez 1094 varnish, achieving a high level of cleanliness, as evidenced by spectrophotometric analysis and optical microscopy observations. Gel 3 (methyl stearate) yielded the best results for oil canvases coated with microcrystalline wax, while Gels 1, 3, and 7 performed best for oil canvases coated with Regalrez 1094. Similarly, Gel 3 yielded the best results for acrylic canvases coated with both microcrystalline wax and Regalrez 1094 varnish.

Methyl stearate gel emerges as the best cleaning system for removing low-polarity materials such as microcrystalline wax and synthetic varnish (Regalrez 1094). It produced excellent chromatic results and left no solvent residue on the surface after the passage with a dry cotton swab.

This research contributes to the ongoing efforts in the cultural heritage conservation field to adopt sustainable practices, aligning with global initiatives for an eco-friendlier approach to artifact restoration.

Author Contributions: Conceptualization, A.M. and C.Z.; methodology, A.M., M.F.L.R. and T.d.C.; software, F.P. and M.F.L.R.; validation, T.d.C. and I.A.C.; formal analysis, C.Z., A.M. and H.A.; investigation, C.Z., A.M., L.M. and F.I.B.; resources, A.M. and M.F.L.R.; data curation, C.Z. and F.I.B.; writing—original draft preparation, C.Z. and A.M.; writing—review and editing, A.M., T.d.C. and F.P.; supervision, A.M. All authors have read and agreed to the published version of the manuscript.

Funding: This research received no external funding.

Institutional Review Board Statement: Not applicable.

Informed Consent Statement: Not applicable.

Data Availability Statement: Data are contained within the article.

Conflicts of Interest: The author Camilla Zaratti was employed by company Lab4green. The remaining authors declare that the research was conducted in the absence of any commercial or financial relationships that could be construed as a potential conflict of interest.

References

1. Macchia, A.; Sacco, F.; Morello, S.; Prestileo, F.; La Russa, F.M.; Ruffolo, S.; Luvidi, L.; Settimo, G.; Rivaroli, L.; Tabasso, M.L.; et al. Quale Sostenibilit  per il Restauro? Chemical Exposure in Cultural Heritage Restoration: Questionnaire to Define the State of the Art. Available online: www.arcadiaricerche.eu (accessed on 23 September 2023).
2. Mangotra, A.; Singh, S.K. Volatile organic compounds: A threat to the environment and health hazards to living organisms—A review. *J. Biotechnol.* **2024**, *382*, 51–69. [[CrossRef](#)] [[PubMed](#)]
3. Phenix, A.; Sutherland, K. The cleaning of paintings: Effects of organic solvents on oil paint films. *Stud. Conserv.* **2001**, *46*, 47–60. [[CrossRef](#)]
4. Pilz, M.; R mich, H. Sol-Gel Derived Coatings for Outdoor Bronze Conservation. *J. Sol-Gel Sci. Technol.* **1997**, *3*, 1071–1075. [[CrossRef](#)]
5. Singhal, D. Cleaning of Textile Artifacts in Museums. 2020. Available online: <https://www.researchgate.net/publication/342231858> (accessed on 25 September 2023).
6. Poulis, J.A.; Mosleh, Y.; Cansell, E.; Cimino, D.; Ploeger, R.; de la Rie, E.R.; McGlinchey, C.W.; Seymour, K. Mechanical and physical characterization of natural and synthetic consolidants. *Int. J. Adhes. Adhes.* **2021**, *117*, 103015. [[CrossRef](#)]
7. Baglioni, P.; Chelazzi, D.; Giorgi, R.; Poggi, G. Colloid and Materials Science for the Conservation of Cultural Heritage: Cleaning, Consolidation, and Deacidification. *Langmuir* **2013**, *29*, 5110–5122. [[CrossRef](#)] [[PubMed](#)]
8. Favaro, M.; Mendichi, R.; Ossola, F.; Russo, U.; Simon, S.; Tomasin, P.; Vigato, P.A. Evaluation of polymers for conservation treatments of outdoor exposed stone monuments. Part I: Photo-oxidative weathering. *Polym. Degrad. Stab.* **2006**, *91*, 3083–3096. [[CrossRef](#)]
9. Letardi, P.; Y n ez-Casal, A. Testing New Coatings for Outdoor Bronze Monuments: A Methodological Overview. *Coatings* **2021**, *11*, 131. [[CrossRef](#)]

10. Shedlosky, T.J.; Huovinen, A.; Webster, D.; Bierwagen, G. Development and Evaluation of Removable Protective Coatings on Bronze. 2004. Available online: www.nma.gov.au (accessed on 25 September 2023).
11. Mitchell, M.R.; Link, R.E.; Crowley, A.; Laefer, D.F.; Fanning, M. Sample Preparation and Testing Methods for the Evaluation of Microcrystalline Waxes for the Seismic Protection of Art Objects. *J. Test. Eval.* **2008**, *36*, 24–33. [[CrossRef](#)]
12. Molina, M.T.; Cano, E.; Ramírez-Barat, B. Protective coatings for metallic heritage conservation: A review. *J. Cult. Heritage* **2023**, *62*, 99–113. [[CrossRef](#)]
13. Cano, E.; Lafuente, D. Corrosion inhibitors for the preservation of metallic heritage artefacts. In *Corrosion and Conservation of Cultural Heritage Metallic Artefacts*; Elsevier: Amsterdam, The Netherlands, 2013; pp. 570–594. [[CrossRef](#)]
14. Kubick, L.; Giaccai, E. Article: A Comparative Study of Protective Coatings for Marble Sculpture. 2000. Available online: www.conservation-us.org (accessed on 26 September 2023).
15. Armal, F.; Dias, L.; Mirão, J.; Pires, V.; Sitzia, F.; Martins, S.; Costa, M.; Barrulas, P. Chemical Composition of Hydrophobic Coating Solutions and Its Impact on Carbonate Stones Protection and Preservation. *Sustainability* **2023**, *15*, 16135. [[CrossRef](#)]
16. Bierwagen, G.; Shedlosky, T.J.; Stanek, K. Developing and testing a new generation of protective coatings for outdoor bronze sculpture. *Prog. Org. Coatings* **2003**, *48*, 289–296. [[CrossRef](#)]
17. Passaretti, A.; Cuvillier, L.; Sciutto, G.; Guilminot, E.; Joseph, E. Biologically Derived Gels for the Cleaning of Historical and Artistic Metal Heritage. *Appl. Sci.* **2021**, *11*, 3405. [[CrossRef](#)]
18. Chelazzi, D.; Bordes, R.; Giorgi, R.; Holmberg, K.; Baglioni, P. The use of surfactants in the cleaning of works of art. *Curr. Opin. Colloid Interface Sci.* **2020**, *45*, 108–123. [[CrossRef](#)]
19. Carretti, E.; Giorgi, R.; Berti, D.; Baglioni, P. Oil-in-Water Nanocontainers as Low Environmental Impact Cleaning Tools for Works of Art: Two Case Studies. *Langmuir* **2007**, *23*, 6396–6403. [[CrossRef](#)]
20. Hellen, R. Preliminary study into the reduction and removal of naturally aged varnishes from painted surfaces using an Er:YAG laser in a two-step cleaning process with solvents. *J. Inst. Conserv.* **2020**, *43*, 79–93. [[CrossRef](#)]
21. Yiming, J.; Sciutto, G.; Prati, S.; Catelli, E.; Galeotti, M.; Porcinai, S.; Mazzocchetti, L.; Samorì, C.; Galletti, P.; Giorgini, L.; et al. A new bio-based organogel for the removal of wax coating from indoor bronze surfaces. *Heritage Sci.* **2019**, *7*, 34. [[CrossRef](#)]
22. Breil, C.; Meullemiestre, A.; Vian, M.; Chemat, F. Bio-Based Solvents for Green Extraction of Lipids from Oleaginous Yeast Biomass for Sustainable Aviation Biofuel. *Molecules* **2016**, *21*, 196. [[CrossRef](#)] [[PubMed](#)]
23. Prasad, W.; Wani, A.D.; Khamrui, K.; Hussain, S.A.; Khetra, Y. Green solvents, potential alternatives for petroleum based products in food processing industries. *Clean. Chem. Eng.* **2022**, *3*, 100052. [[CrossRef](#)]
24. Radzi, S.M.; Basri, M.; Salleh, A.B.; Ariff, A.; Mohammad, R.; Rahman, M.B.A.; Rahman, R.N.Z.R.A. High performance enzymatic synthesis of oleyl oleate using immobilised lipase from *Candida antarctica*. *Electron. J. Biotechnol.* **2005**, *8*, 291–298. [[CrossRef](#)]
25. Smith, G.D.; Johnson, R. Strip ‘Teas’-Solubility Data for the Removal (and Application) of Low Molecular Weight Synthetic Resins Used as Inpainting Media and Picture Varnishes. *WAAC Newsl.* **2008**, *30*, 11–19.
26. Hans, P. Regalrez in Furniture Conservation. *J. Am. Inst. Conserv.* **2001**, *40*, 59.
27. Fernandes, C.C.; Haghbakhsh, R.; Marques, R.; Paiva, A.; Carlyle, L.; Duarte, A.R.C. Evaluation of Deep Eutectic Systems as an Alternative to Solvents in Painting Conservation. *ACS Sustain. Chem. Eng.* **2021**, *9*, 15451–15460. [[CrossRef](#)]
28. Baij, L.; Hermans, J.; Ormsby, B.; Noble, P.; Iedema, P.; Keune, K. A review of solvent action on oil paint. *Heritage Sci.* **2020**, *8*, 43. [[CrossRef](#)]
29. Stefanis, E.; Panayiotou, C. Prediction of Hansen Solubility Parameters with a New Group-Contribution Method. *Int. J. Thermophys.* **2008**, *29*, 568–585. [[CrossRef](#)]
30. Vay, K.; Scheler, S.; Frieß, W. Application of Hansen solubility parameters for understanding and prediction of drug distribution in microspheres. *Int. J. Pharm.* **2011**, *416*, 202–209. [[CrossRef](#)] [[PubMed](#)]
31. Macchia, A.; Rivaroli, L.; Gianfreda, B. The GREEN RESCUE: A ‘green’ experimentation to clean old varnishes on oil paintings. *Nat. Prod. Res.* **2019**, *35*, 2335–2345. [[CrossRef](#)] [[PubMed](#)]
32. Raza, Z.A.; Abid, S.; Banat, I.M. Polyhydroxyalkanoates: Characteristics, production, recent developments and applications. *Int. Biodeterior. Biodegrad.* **2018**, *126*, 45–56. [[CrossRef](#)]
33. Adnan, M.; Siddiqui, A.J.; Ashraf, S.A.; Snoussi, M.; Badraoui, R.; Alreshidi, M.; Elsbali, A.M.; Abu Al-Soud, W.; Alharethi, S.H.; Sachidanandan, M.; et al. Polyhydroxybutyrate (PHB)-Based Biodegradable Polymer from *Agromyces indicus*: Enhanced Production, Characterization, and Optimization. *Polymers* **2022**, *14*, 3982. [[CrossRef](#)] [[PubMed](#)]
34. Cairns, L.K.; Forbes, P.B.C. Insights into the yellowing of drying oils using fluorescence spectroscopy. *Heritage Sci.* **2020**, *8*, 1–11. [[CrossRef](#)]
35. De Winter, S. Conservation Problems with Paintings Containing Fluorescent Layers of Paint. CeROArt (Conservation, Exposition, Restauration d’Objets d’Art), no. EGG 1, 2010. OpenEdition Journals. Available online: <https://journals.openedition.org/ceroart/1659> (accessed on 26 September 2023).

36. Bacci, M.; Ciatti, F.M. Società Italiana di Ottica e Fotonica Gruppo di Lavoro in Colorimetria e Reflectoscopia Colorimetria e Beni Culturali Atti dei Convegni di Firenze 1999 e Venezia 2000 col Patrocinio di: Istituto Centrale di Restauro Progetto beni Culturali-CNR. Available online: <https://findit-uat.library.yale.edu/catalog/digcoll:2784391> (accessed on 27 September 2023).
37. Del Grosso, C.A.; Poulis, J.A.; de la Rie, E.R. The photo-stability of acrylic tri-block copolymer blends for the consolidation of cultural heritage. *Polym. Degrad. Stab.* **2019**, *159*, 31–42. [CrossRef]

Disclaimer/Publisher’s Note: The statements, opinions and data contained in all publications are solely those of the individual author(s) and contributor(s) and not of MDPI and/or the editor(s). MDPI and/or the editor(s) disclaim responsibility for any injury to people or property resulting from any ideas, methods, instructions or products referred to in the content.